ON FATIGUE CRACK INITIATION AND PROPAGATION AT ELEVATED TEMPERATURE

H. Teranishi* and A. J. McEvily**

*Formerly Research Associate, is now with
Sumitomo Metals, Inc., Amagasaki, Japan
**Professor, Metallurgy Dept., Institute of Materials Science,
University of Connecticut, Storrs, CT 06268

INTRODUCTION

The low cycle fatigue resistance of steels at elevated temperatures will depend upon a number of factors including crystal structure, alloy chemistry and processing history. Each of these variables can influence strength and ductility as well as creep and oxidation resistance and thereby affect fatigue properties. The purpose of the present study is to determine microstructural influences on low cycle, elevated temperature fatigue behavior by comparing two austenitic alloys, Alloy 800 and 800 H with two ferritic alloys, 2 1/4 Cr-1 Mo and 2 1/4Cr-1Mo-V. Attention is given to the determination of the number of cycles to initiate a 0.1 mm crack as well as to the effects of oxidation, particularly when hold times are included in the loading cycle.

MATERIAL

Table 1 lists the chemical compositions of the four alloys tested. Alloy 800 and Alloy 800 H were tested at 500°C and 650°C. The 2 1/4Cr-1Mo alloys were tested at 593°C. The mechanical properties at room temperature and the elevated test temperatures are listed in Table 2. The footnotes provide processing details. Hourglass fatigue specimens as shown in Fig. 1 were used in these tests. The average strain rate was generally 4×10^{-3}/sec. Tests were run under total diametral strain control and the width of the hysteresis loop at zero load at saturation was used to obtain the inelastic strain range, $\Delta\varepsilon_p$. In a few of the tests a ten minute hold time either in tension or compression, was introduced into each cycle in order to determine the effect of such a hold time on fatigue life. In presenting the results all diametral strains have been converted to equivalent longitudinal strains. The elevated temperature fatigue tests were carried out in a servo-hydraulic closed loop fatigue test system equipped with an induction heater.

RESULTS AND DISCUSSION

The results of the fatigue tests are given in Table 3. In the cyclic tests both the 2 1/4 Cr-Mo alloys underwent cyclic softening at 593°C (1). Alloy 800 and Alloy 800 H both cyclically hardened at both 500°C and 650°C (2). For alloy 800 the saturation stress for a total strain range, $\Delta\varepsilon_t$, of 1% was less than at room temperature, whereas for alloy 800 H, the saturation stress was higher than at room temperature due to the precipitation of carbides (3). Saturation stress for

the Cr-Mo steels at 593°C were less than the corresponding room temperature values.

The fatigue results are shown in Fig. 2 as a function of inelastic strain range $\Delta\varepsilon_p$. It is noted that there is a trend for the highest strength materials to exhibit the lowest fatigue strength. On the other hand if the results are plotted in terms of the saturation stress range, $\Delta\sigma$, as in Fig. 3 then the highest strength materials tend to show the best fatigue behavior. In order to combine the influence of both stress and strain, a single parameter, $\Delta\sigma\,\Delta\varepsilon_p$, can be used. Fatigue lifetimes plotted against this parameter are shown in Fig. 4. It is seen that this parameter provides a reasonable degree of correlation of the test results at high cyclic strain rates of 4×10^{-3} per second.

The effect of a hold time on fatigue behavior is shown in Fig. 5. For purposes of comparison at a single temperature, 593°C, the 500 and 650°C results for Alloy 800 and 800 H have been linearly interpolated. This figure shows that a hold time in compression is more damaging than a hold time in tension for the Cr-Mo alloys whereas the reverse is true for Alloy 800. This circumstance has been shown to be due to the behavior of the oxide formed during the hold period on the Cr-Mo alloys. This oxide spalls from the specimen surface after a tension hold, leaving behind a relatively smooth surface. On the other hand, after a hold in compression the oxide cracks rather than spalls to create a surface as in Fig. 6. As a result fatigue cracks are more readily created and the lifetime is lessened. In the case of austenitic alloy, although oxidation does occur as easily seen by the bluish film which forms on the specimen surfaces, the oxide is much more adherent and less easily cracked. Since no obvious creep damage was observed i.e., cavitation along the grain boundaries, the damaging effect of the tensile hold may simply be to increase the plastic strain range by stress relaxation and thereby lessen fatigue life. In addition, as will be discussed the greater time allowed for additional oxidation during the hold also contributes to a lower fatigue lifetime.

After fatigue testing to failure the fracture surfaces were examined in a Scanning Electron Microscope. Crack growth paths were generally transgranular, although evidence of intergranular fracture was found in Alloy 800 tested at 650°C at a slow strain rate 4×10^{-5}/sec. This alloy contained patches of large (40μm) and small (5μm) grains, an effect due to processing. In general fatigue striations were evident on the fracture surfaces and by measuring the spacings of the striations starting from the outer most, a plot of crack length versus number of cycles can be constructed (4,5). Results for each material are shown in Fig. 7 for continuous cycling as well as for hold time tests. From Fig. 7 an estimate of the number of cycles to form a crack 0.1 mm in length can be made and Fig. 8 compares the various alloys on this basis. As is usually observed the greater the strain range the smaller the percentage of life to initiate a crack. It is also seen that cracks initiate earlier in life in the case of the Cr-Mo steels than for Alloy 800. In the latter case an increase in temperature leads to earlier initiation of cracks as a percentage of total lifetime. These resutls are interpretable in terms of oxidation resistance. The greater the amount of oxide formed the sooner in life will cracks develop.

It is of interest to compare the rate of crack growth as determined from the fatigue striation spacing with predicted values (6). This comparison is done in Table 4 and quite good agreement is found. This may be somewhat surprising since the predictions are based on purely mechanical considerations and do not take oxidation effects into account. However for these macrocracks, the advance per cycle can be considered to be the sum of an increment due to sliding off plus an increment due to oxidation. Where the former is larger than the latter, mechanical considerations will govern. Since the time per cycle is but a few seconds, not much oxidation at the growing macrocrack tip can occur which may account for the good agreement between predicted and experimental values. This situation will change during micro-crack growth at the fatigue crack origin, for there the advance

per cycle will be much less and the environmental effect can dominate. Lower test frequencies and hold times will also promote environmental influences, as can be seen from Fig. 7. In this case a ten minute hold time approximately doubles the rate of crack growth for Alloy 800, but much more significantly increases the crack growth rate for the Cr-Mo alloys. In fact, if in Fig. 7, one extrapolates to a crack length at zero cycles, it appears that hold times reduce this crack length. This extrapolated crack length may represent the length of crack at which the growth process changes from a microstructure sensitive mechanism to a continuum mechanism. The formation of an easily cracked oxide would increase the notch sensitivity of the material and promote this transition.

CONCLUDING REMARKS

1. At elevated temperatures the relative oxidation resistance of alloys will obviously influence comparisions of fatigue behavior. The effects of oxidation, a time dependent process, will be most pronounced in low frequency tests involving hold times.
2. Oxidation promotes the early initiation of cracks and can influence crack growth rates to an extent which depends upon the relative contribution to each growth increment of mechanical and environmental factors.
3. The parameter, $\Delta\sigma\,\Delta\varepsilon_p$, has been found to be useful in comparing the fatigue behavior of different alloys at elevated temperature.

ACKNOWLEDGEMENT

The authors express their appreciation to Huntington Alloys for supplying Alloy 800 and Alloy 800 H and to the Climax Molybdenum Corporation of Michigan for the Cr-Mo alloys. The support of the AMAX Foundation is also gratefully acknowledged as is the assistance of Dr. V.M. Radhakrishnan for his excellent help in preparing the manuscript.

REFERENCES

1. Teranishi H. and A. J. McEvily (1979). Proc. Inter. Symposium on Low Cycle Fatigue Strength. DVM. p. 25, Eds. Rie and Haibach.
2. Teranishi, H. and A. J. McEvily (1979). Fatigue of Eng. Mat. & Struc., Vol. 2 p. 289.
3. Teranishi, H. and A. J. McEvily (1978). Proc. Alloy 800, ed. W. Betteridge North-Holland Publishing Company, p. 125.
4. Ermi, A.M., H. Nahm and J. Moteff (1977). Mater. Sci. Eng., Vol. 30, p. 41.
5. Maiya, P.S. (1975). Scripta Met., Vol. 9, p. 1141.
6. Wareing, J. and H. G. Vaughan (1977). Met. Sci., Vol. 11, p. 439.

TABLE 1. Chemical Composition

ALLOY	C	Mn	Si	S	Cu	Ni	Cr	Ti	Al	N	Ti C+N
800	0.03	0.93	0.28	0.007	0.5	32.43	20.55	0.41	0.42	0.015	9.1
800H	0.07	0.77	0.39	0.004	0.49	33.43	20.36	0.46	0.43	0.015	5.4

ALLOY	C	Mn	Si	S	N	Sn	As	Sb	V
2¼Cr-1Mo	0.13	0.40	0.21	0.015	0.008	0.009	0.009	0.002	0.00
2¼Cr-1Mo-V	0.12	0.43	0.23	0.016	0.009	0.008	0.008	0.003	0.28

TABLE 2. Mechanical Properties

ALLOY	Temp. °C	0.2% YS MPa	UTS MPa	% Elongation	% Area Reduction	Grain Size ASTM
2¼Cr-1Mo*	RT	470	597	20.0	77.7	
	593	305	354	34.5	87.0	
2¼Cr-1Mo-V*	RT	620	720	18.0	74.6	
	593	443	456	26.5	82.4	
800**	RT	228.4	592.7	42	79.1	
	500	151	505.8	46	69.1	
	650	129	414.7	41	52.1	5
800H***	RT	198	584.4	45	71.3	
	500	116	523.7	57	61.6	3.5
	650	119.4	460	48	64.0	

* Austenitized at 955°C, 1 hour, air cooled, followed by tempering at 730°C for two hours and air cooled. Before testing the microstructure of the alloy, 2¼Cr-1Mo consisted of ferrite and bainite; that of the 2¼Cr-1Mo-V alloy consisted of bainite. The hardness of the bainite phase decreased from 230 to 200 DPH after testing at 593°C.

** 968°C mill anneal

*** 1149°C solution treated

TABLE 3. Results of Fatigue Testing

Alloy 2-1/4Cr-1Mo

Specimen Number	Temp. °C	$\Delta\varepsilon_t$ (%)	$\Delta\varepsilon_p$ (%)	$\Delta\varepsilon_e$ (%)	$\dot{\varepsilon}$ (/sec) x10^{-3}	$\Delta\sigma$ (MPa)	N_f (Cycles)
1	R.T.	1.027	0.560	0.467	4.21	760	6091
2	593	0.523	0.256	0.267	4.18	478	7179
3		0.544	0.285	0.259	4.34	436	5100
4		0.773	0.460	0.313	4.12	478	2980
5 **		0.840	0.740	0.100	3.36	492	799
6 *		0.860	0.700	0.160	3.44	402	1065+
7		0.920	0.520	0.400	3.68	498	2647
8		0.927	0.660	0.267	14.80	520	2699
9		0.973	0.760	0.213	0.39	450	1623
10		0.993	0.660	0.313	4.12	450	2443
11		1.410	1.100	0.310	3.76	492	1109
12		1.840	1.540	0.300	3.68	510	777
13		2.330	1.980	0.330	3.68	582	555

* Tension hold testing with hold time 10 minutes.
** Compression hold testing with hold time 10 minutes.
\+ Test was terminated due to excessive reduction of the diameter (because of the oxide scale spalling).

Alloy 2-1/4Cr-1Mo-V

Specimen Number	Temp. °C	$\Delta\varepsilon_t$ (%)	$\Delta\varepsilon_p$ (%)	$\Delta\varepsilon_e$ (%)	$\dot{\varepsilon}$ (/sec) x10^{-3}	$\Delta\sigma$ (MPa)	N_f (Cycles)
1	R.T.	1.019	0.472	0.547	4.07	986	4977
2	593	0.557	0.224	0.333	4.46	535	5072
3		0.571	0.224	0.347	4.60	591	4645
4		0.813	0.380	0.433	4.34	634	2734
5**		0.933	0.700	0.233	3.72	622	505
6*		0.940	0.740	0.200	3.76	536	1201
7		0.984	0.624	0.360	3.94	680	301+
8		1.024	0.624	0.400	4.10	613	1904
9		1.027	0.560	0.467	10.27	632	2159
10		1.040	0.640	0.400	0.42	470	1519
11		1.400	1.100	0.300	3.73	620	861
12		1.900	1.500	0.400	3.80	685	605

* Tension hold testing with hold time 10 minutes
** Compression hold testing with hold time 10 minutes
\+ Failed at the place where the thermocouples were spot welded.

TABLE 3. Results of Fatigue Testing (Continued)

Alloy 800

Specimen Number	Temp. (°C)	$\Delta\varepsilon_t$ (%)	$\Delta\varepsilon_p$ (%)	$\Delta\varepsilon_e$ (%)	$\dot{\varepsilon}$ (/sec) x10^{-3}	$\Delta\sigma$ (MPa)	N_f cycles
1	R.T.	0.955	0.568	0.387	3.82	697	7205
2	500	0.485	0.112	0.373	3.88	513.4	75313
3		0.724	0.352	0.372	3.86	580.0	8200
4		0.793	0.360	0.433	4.24	590	8141
5		0.971	0.544	0.427	3.88	618	5588
6		0.978	0.533	0.444	3.91	624	5935
7		1.467	0.900	0.567	3.90	759	1703
8		1.440	0.906	0.533	3.83	737	2284
9		1.950	1.280	0.670	3.89	844	732
10		1.902	1.280	0.622	3.80	900	555
11		1.030	0.496	0.533	1.24	633	5519
12		1.020	0.512	0.507	0.41	646	4052
13		1.087	0.420	0.667	0.044	759	1350
14	650	0.740	0.380	0.360	3.90	570	3053
15		1.010	0.610	0.400	4.04	607	2212
16		1.460	1.060	0.400	3.90	606	745
17		1.840	1.340	0.500	3.70	703	520
18		1.140	0.840	0.300	0.046	607	388

Alloy 800-H

Specimen Number	Temp. (°C)	$\Delta\varepsilon_t$ (%)	$\Delta\varepsilon_p$ (%)	$\Delta\varepsilon_e$ (%)	$\dot{\varepsilon}$ (/sec) x10^{-3}	$\Delta\sigma$ (MPa)	N_f cycles
1	R.T.	0.980	0.520	0.460	3.92	660	15176
2	500	0.484	0.128	0.356	3.87	575	32619
3		0.672	0.299	0.373	3.84	700	9842
4		0.796	0.299	0.498	4.25	700	8800
5		1.017	0.501	0.516	4.06	787	4024
6		1.485	0.907	0.578	3.95	900	1515
7		1.950	1.280	0.667	3.89	1002	356
8		1.028	0.459	0.569	0.411	837	3515
9		1.084	0.373	0.711	0.043	900	2070
10	650	0.530	0.150	0.380	4.20	611	10804
11		0.740	0.300	0.440	3.90	700	3621
12		1.060	0.500	0.560	4.20	742	2003
13		1.520	0.920	0.600	4.00	844	1043
14		1.990	1.320	0.670	4.00	928	516
15		3.560	2.960	0.600	3.60	1012	210
16		1.053	0.720	0.333	0.042	742	458
17*		1.107	0.74				895
18**		0.967	0.70				829

* 10 minutes hold at compression
** 10 minutes hold at tension and compression.

TABLE 4. Comparison of Predicted and Experimental Crack Growth Rates

ALLOY	Temp. °C	β**	T* MPa	σ MPa	$\Delta\varepsilon_p$ %	$\frac{da}{dN}/a$	Ratio calcul. to Experi.
800	500	0.367	505.8	308.4	0.533	1.41×10^{-3}	1.0
	650	0.171	414.7	306.4	0.610	3.06×10^{-3}	1.0
800H	500	0.237	523.7	395.4	0.801	2.39×10^{-3}	1.7
	650	0.179	460.0	376.7	0.500	3.09×10^{-3}	1.0
2¼Cr-Mo	593	0.0814	354	245	0.66	2.71×10^{-3}	1.0
2¼Cr-Mo-V	593	0.0855	456	319.5	0.624	2.61×10^{-3}	1.0

* Tensile strength
** Cyclic hardening exponent

Note that the cyclic strain hardening exponent of the austenitic steel is much larger than that for the ferritic alloy.

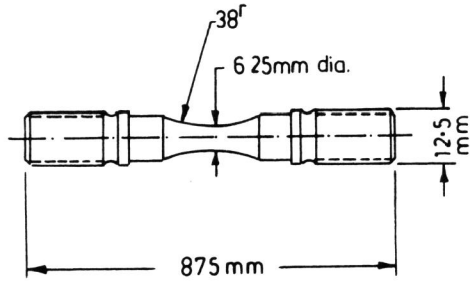

FIG.1. FATIGUE SPECIMEN

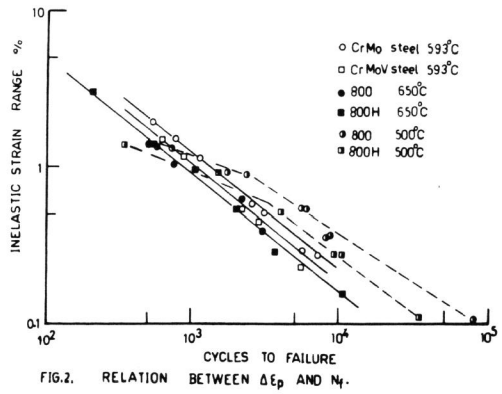

FIG.2. RELATION BETWEEN $\Delta\varepsilon_p$ AND N_f.

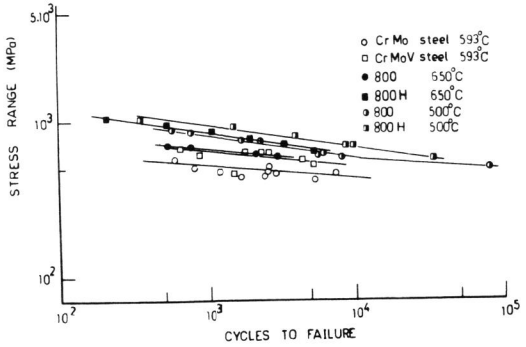

FIG.3. RELATION BETWEEN $\Delta\sigma$ AND N_f

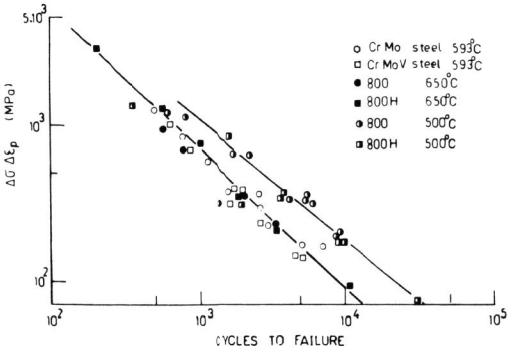

FIG.4. $\Delta\sigma\,\Delta\varepsilon_p$ vs N_f.

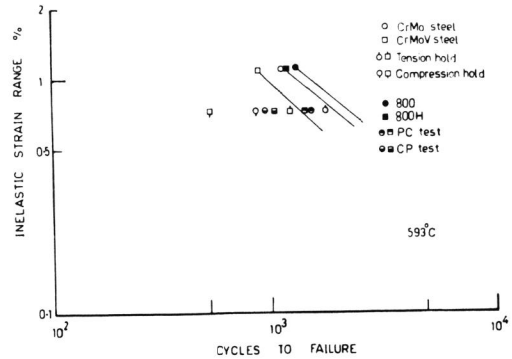

FIG.5. EFFECT OF HOLD TIME ON FATIGUE LIFE.

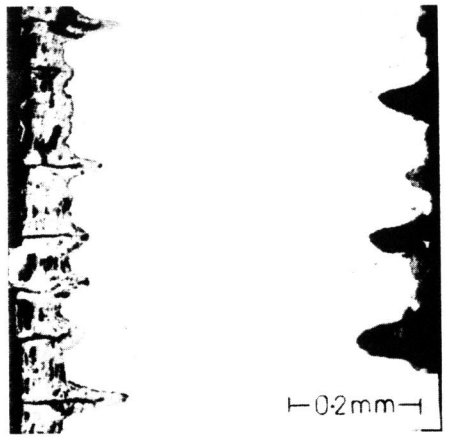

Fig.6. Cracking of Oxide after a hold in Compression.

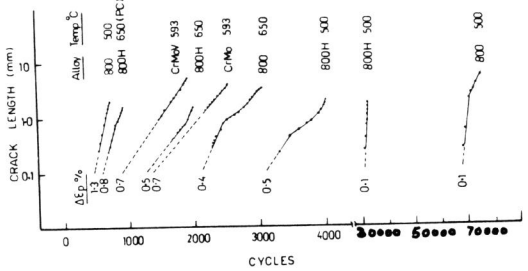

FIG.7. CRACK LENGTH vs CYCLES.

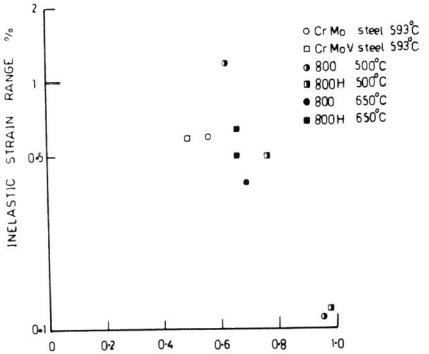

FIG.8. RELATION BETEEN $\Delta\varepsilon_p$ AND N_i/N_f.